# *Interpixel crosstalk in a 3D-integrated active pixel sensor for x-ray detection*

# Interpixel cross-talk in a 3D-integrated active pixel sensor for X-ray detection

Beverly LaMarr[a] Mark Bautz[a], Rick Foster[a], Steve Kissel[a], Gregory Prigohzin[a] and Vyshnavi Suntharalingam[b]

[a]MIT Kavli Institute for Astrophysics and Space Research, 70 Vassar Street, Cambridge, MA USA, 02139;

[b]MIT Lincoln Laboratory, 244 Wood Street, Lexington, MA USA 02420-9108

## ABSTRACT

MIT Lincoln Laboratories and MIT Kavli Institute for Astrophysics and Space Research have developed an active pixel sensor for use as a photon counting device for imaging spectroscopy in the soft X-ray band. A silicon-on-insulator (SOI) readout circuit was integrated with a high-resistivity silicon diode detector array using a per-pixel 3D integration technique developed at Lincoln Laboratory. We have tested these devices at 5.9 keV and 1.5 keV. Here we examine the interpixel cross-talk measured with 5.9 keV X-rays.

**Keywords:** Active pixel sensor (APS), X-ray, cross-talk

## 1. INTRODUCTION

MIT Lincoln Laboratories and the MIT Kavli Institute have been developing a three-dimensionally integrated active pixel sensor (APS) for use in X-ray astronomy.[1] The overall goal of this NASA-supported program is to enable soft X-ray detection with spectral and spatial resolution similar to CCDs but with faster readout speeds, warmer optimal operating temperatures and increased radiation tolerance.

The device is a 256x256 array of 24x24 micron photodiode pixels integrated with an SOI CMOS readout tier. The detector is back-illuminated and the 50-micron thick detector layer is fully depleted. Detailed characterization of this device, including its noise performance, X-ray spectral resolution and depletion depth has been presented elsewhere.[2,3] Here we focus on the interpixel cross-talk, as measured in the X-ray band.

Interpixel cross-talk is especially important in X-ray applications of APS because the signal produced by an X-ray can be shared between neighboring pixels, for example if the X-ray interaction occurs near a pixel boundary. In these cases accurate X-ray spectroscopy requires that the charge in two adjacent pixels be measured. Often these so-called split events will have only a few percent of the total signal charge in the neighboring pixel, so it is important to understand all the sources of cross-talk, including those produced in the device readout circuitry, to obtain the best possible X-ray performance.

## 2. EXPERIMENT AND DATA ACQUISITION

The tests reported here were conducted on multiple devices at temperatures ranging from room temperature to -60C and readout of 156.25 kHz and 312.5 kHz.

We illuminated the device with an $Fe^{55}$ source and are able to resolve the Mn K$\alpha$ line at 5.9 keV and the K$\beta$ line at 6.4 keV.

The device packaging and our setup allow us to illuminate the device from either the front or the back. Tests in both orientations are reported here.

A small number of pixels in a single row are readout during one test. First they're all held in reset. Then, with the reset switch turned off, the chosen pixels were sequentially readout multiple times. Each pixel is sampled

Send correspondence to Beverly LaMarr
E-mail: fergason@space.mit.edu, Telephone: 1 617 258 8153

High Energy, Optical, and Infrared Detectors for Astronomy IV, edited by Andrew D. Holland, David A. Dorn
Proc. of SPIE Vol. 7742, 77422B · © 2010 SPIE · CCC code: 0277-786X/10/$18 · doi: 10.1117/12.857137

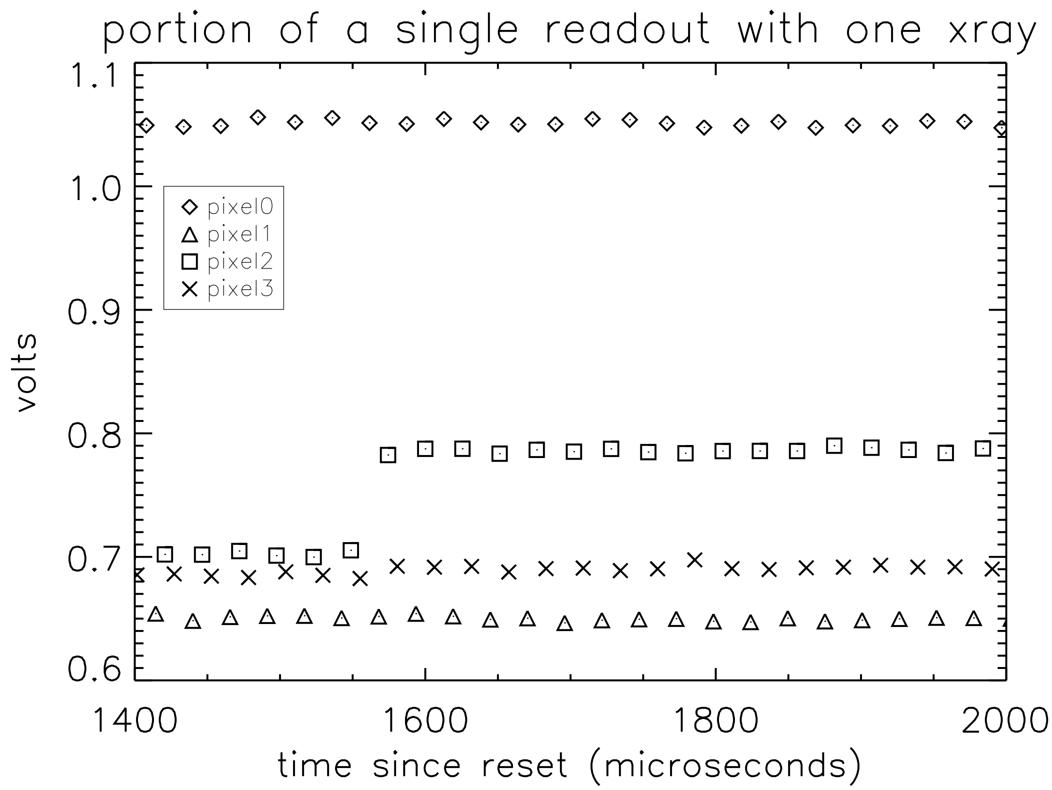


Figure 1. Signals from each of four adacent pixels, plotted as a funciton of time during an X-ray interatciton in one pixel. Each pixel is plotted with a different symbol. Pixels were sampled sequentially, and the X-ray event occurred in pixel 3 at approximately 1550 microseconds. The X-ray was detected in the second pixel 1500 microseconds after the row was reset. The reset level is slightly different for each pixel, left uncorrected here to make the plot easier to read.

without being reset between 65 and 130 times depending on the number of pixels being tested. Such a mode allowed us to apply noise reduction algorithms significantly improving device energy resolutions (see [2]). Most tests were conducted with the column number increasing during the readout but in some the order was reversed.

A portion of the output centered around an x-ray detection is shown in Figure 1.

## 3. ANALYSIS

The amplitude for each x-ray is calculated by subtracting the average of ten samples before the event from the average of ten samples after the event. Processing this way greatly reduces the effects of reset noise and white noise in the system.

A histogram of the amplitudes for a single pixel is shown in Figure 2. The FWHM for the Mn K$\alpha$ peak at 5.9 keV for the set shown is 275 eV, which is typical for data taken in this mode. Better performance has been achieved with this sensor, as reported elsewhere.[2,3]

As noted in the introduction, charge from a single X-ray interaction may be split between two adjacent diodes in the detector tier due to signal charge diffusion. This phenomenon is analogous to charge splitting observed in CCD detectors. Our focus here, however, is on capacitive interpixel cross-talk in the readout circuitry. In order to exclude events which may be affected by charge splitting in the detector tier, we filter the data to include only x-rays in the high energy half of the Mn K$\alpha$ peak (see the dotted vertical lines in Figure 2 which are at the center and center plus 3*sigma).

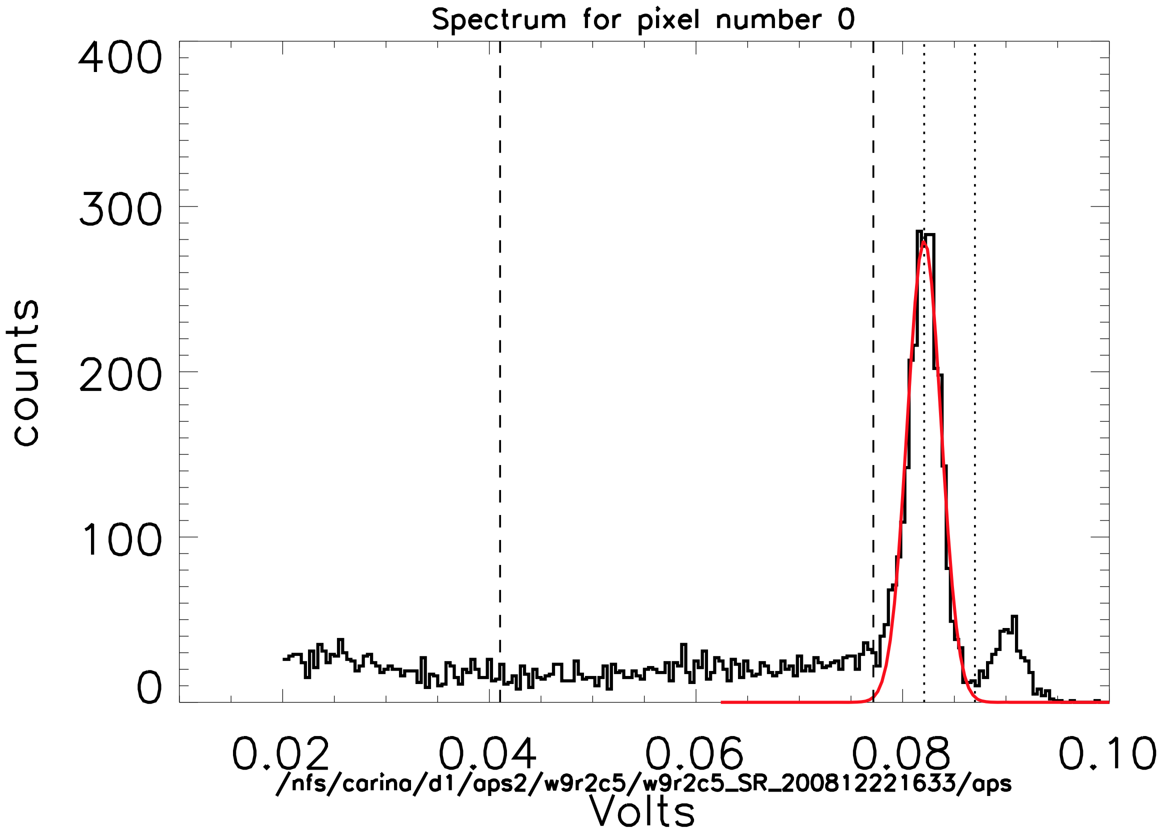


Figure 2. $Fe^{55}$ Spectrum for a single pixel. The data are plotted in black with a gaussian fit to the Mn K$\alpha$ peak overplotted in red. This set was taken at -60C with an $Fe^{55}$ source illuminating the front surface of w9r2c5. Pixel at row 180, column 180 is shown.

Once the desired events have been selected a median clipped average at each time sample preceding and following the X-ray hit is calculated as seen in Figure 3. In these plots the values have been bias corrected to provide the same zero level. The bias was calculated by taking a median of 256 values for each sample at a given time since reset.

The cross-talk amplitudes found to either side of the detected x-ray for several different sets of conditions are summarized in Table 1. The cross-talk to the right is nearly 10% while the cross-talk to the left is an order of magnitude smaller, around 1%.

## 4. DISCUSSION AND CONCLUSIONS

In our APS2 devices we are able to measure interpixel cross-talk using X-rays. After removing events where the charge is split due to carrier diffusion in the detector tier, we find a significant asymmetry in the cross-talk amplitude.

A likely explanation for the asymmetric cross-talk is suggested by examination of the pixel readout tier layout, seen in Figure 4. The via that is connected to the floating sense node is located close to the output of the source follower of the adjacent pixel on the left. Thus, when signal appears at the sense node of the pixel on the left, its source follower output affects the nearby floating sense node on the right through a capacitive link, producing a cross-talk signal (for more details on the pixel schematic see [2,3]). On the other hand, when signal appears in the central pixel sense node, it does not result in a similar crosstalk in the left side pixel, because the output of the left side source follower is not floating, its voltage level being determined by conductivities of its transistors.

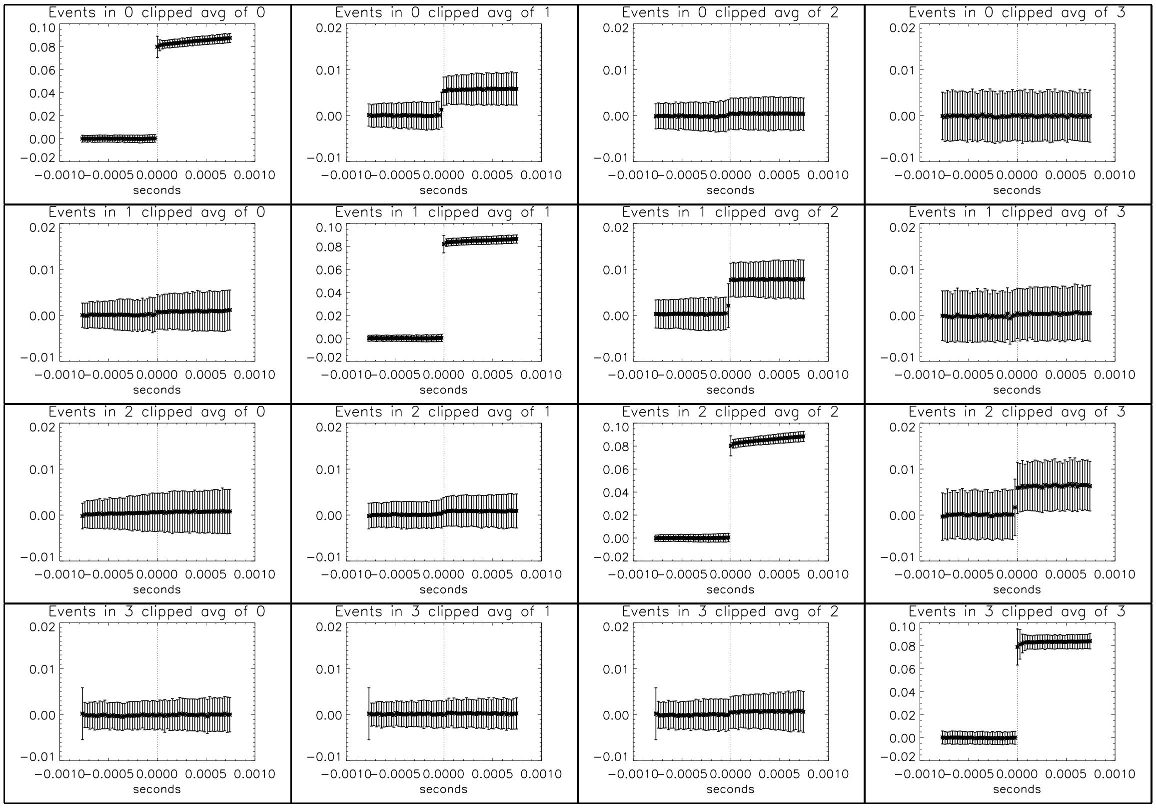


Figure 3. Average trace for un-split events. Each point is the average of all values below the median plus 4*sigma for the sample. The error bars are the standard deviation of the remaining values. Notice that the scale for the x-ray (the plots on the diagonal) is different from the rest. This set was taken at -60C with an $Fe^{55}$ source illuminating the front surface of w9r2c5. Pixels at row 180, columns 180 through 183 are shown.

| device | pixel | column order | clock speed (kHz) | illuminated surface | temperature | left cross-talk (%) | right cross-talk (%) |
|---|---|---|---|---|---|---|---|
| w9r2c5 | c181r180 | increasing | 156.25 | front side | -60C | 0.9 | 8.9 |
| w9r2c5 | c182r180 | increasing | 156.25 | front side | -60C | 1.0 | 7.4 |
| w9r2c5 | c181r180 | decreasing | 156.25 | front side | -60C | 0.8 | 8.9 |
| w9r2c5 | c182r180 | decreasing | 156.25 | front side | -60C | 0.8 | 7.2 |
| w9r2c5 | c181r180 | increasing | 156.25 | front side | -60C | 1.4 | 7.3 |
| w9r2c5 | c182r180 | increasing | 156.25 | front side | -60C | 0.4 | 7.6 |
| w9r2c5 | c183r180 | increasing | 156.25 | front side | -60C | 0.8 | 8.7 |
| w9r2c5 | c184r180 | increasing | 156.25 | front side | -60C | 1.1 | 6.7 |
| w9r2c5 | c185r180 | increasing | 156.25 | front side | -60C | 0.6 | 9.3 |
| w9r2c5 | c186r180 | increasing | 156.25 | front side | -60C | 1.5 | 7.2 |
| w8r5c3 | c33r154 | increasing | 312.5 | back side | room temp | 0.6 | 6.9 |
| w8r5c3 | c34r154 | increasing | 312.5 | back side | room temp | 0.6 | 6.0 |

Table 1. Cross-talk relative to event amplitude for various setups.

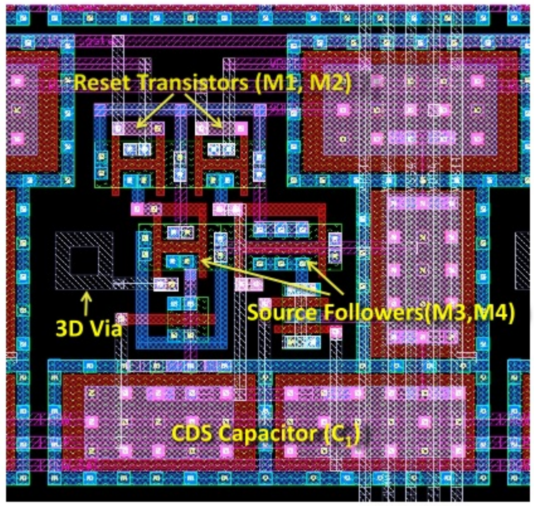


Figure 4. Layout of APS2 pixel readout tier.

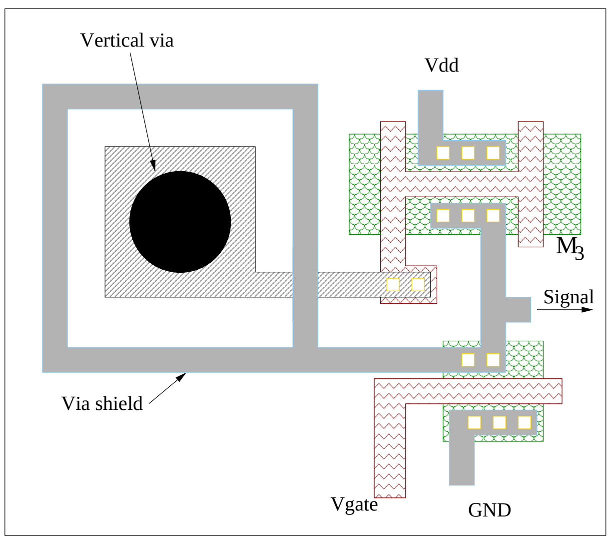


Figure 5. Proposed pixel layout

This mechanism suggests a possible solution that can significantly reduce the interpixel crosstalk. If the sense node is encircled by a metal line that is connected to the output of its own source follower, the sense node will be shielded from the adjacent pixels' source followers, and corresponding capacitive couplings would be greatly reduced. Such a shield adds very little to the sense node capacitance since its voltage follows the voltage a the sense node with a gain that is very close to one. A pixel topology of such an arrangement is shown schematically in Figure 5.

## ACKNOWLEDGMENTS

This work was funded by the NASA grant number NNG06WC08G.

## REFERENCES

[1] Suntharalingam, V., Rathman, D., Prigozhin, G., Kissel, S., and Bautz, M., "Back-Illuminated three-dimentionally integrated CMOS image sensors for scientific applications," *SPIE Proceedings, Focal Plane Arrays for Space Telescopes* **6690** (2007).

[2] Prigozhin, G., Suntharalingam, V., Busacker, D., Foster, R., Kissel, S., LaMarr, B., Soares, A., Villasenor, J., and Bautz, M., "Characterization of 3D-integrated Active Pixel Sensor for X-ray Detection," *IEEE Transactions on Electron Devices* **ED-56**(11), 2602–2611 (2009).

[3] Prigozhin, G. Y., Foster, R. F., Suntharalingam, V., Kissel, S. E., LaMarr, B. J., and Bautz, M. W., "Measurement results for an x-ray 3d-integrated active pixel sensor," *SPIE Proceedings, High Energy, Optical, and Infrared Detectors for Astronomy IV* **7742**, these procedings (2010).